Sustainable

Engineering and Technological Sciences

https://sets.zenithacademic.co.uk/index.php/sets/index

Sustainable Engineering and Technological Sciences, 01(01), 2025, pp. 71-81

DOI: https://doi.org/10.70516/8tk3qp78

ISSN 3049-7787 (Print)
ISSN 3049-7795 (Online)

Breakage Time of Bubble in a Stirred Tank for Different Impeller Geometries, An Experimental Investigation

Muayad F. Hamad[1,a*], Basim O. Hasan[1,b], Hasan Sh. Majdi[2,c], Abbas Al-Farraji[1,d]

[1] Department of Chemical Engineering, Al-Nahrain University, Baghdad, Iraq
[2] Department of Chemical Engineering and Petroleum Industries, Al-Mustaqbal University College, Babil, Iraq.

[a] Corresponding author's email: muayad.f.hamad@nahrainuniv.edu.iq (https://orcid.org/0000-0003-4067-159X)
[b] basim.o.hasan@nahrainuniv.edu.iq (https://orcid.org/0000-0001-6774-562X)
[c] hasanshker1@gmail.com (https://orcid.org/0000-0001-7871-9048)
[c] abbas.m.abdulkareem@nahrainuniv.edu.iq (https://orcid.org/0000-0001-5327-8581)

Article info

Received 15 September 2024

Revised 8 December 2024

Accepted 10 December 2024

Available online 1 January 2025

Keywords: *Breakup Time; Impeller Geometry; Stirred Tank; Breakup Probability; Birth Rate.*

Abstract. The successful tank stirring operation requires extensive studies for selecting a suitable impeller design for the dispersion processes in such systems. In this context, the effects of impeller geometry and Reynolds number (Re) on bubble breakage time were investigated to gain a deeper understanding of the breakage phenomena. Three different impeller geometries were investigated: a 4-Twisted blades impeller (4TB), a 4-Flat blades impeller (4FB), and a 2-Flat blades impeller (2FB) For Re range of 18380 to 40830 (based on impeller diameter). Three different time intervals were recognized during the mother bubble's motion; initial breakage time, final breakage time, and retention time. The initial and final breakage times were calculated by following the injected bubble using a high speed camera at different zones around and in the impeller region. It was found that the breakage time decreases with increasing Reynolds number (or stirring speed) for all geometries. The 4-Flat blades impeller showed the lowest breakage time indicating the highest breakage rate. For 4-FB impeller, it decreases by about 20% when the Re increases from 18380 to 40830. The breaking interval increases with increasing Re and is lowest for 4FB impeller. The increase is for 4FB is 65%.

1. Introduction

Dispersion phenomena is a case widely encountered in industrial applications such as bioreactors, two phase mixing, separation processes in petroleum industry, extractions, etc. The characterization of breakage behavior of fluid particles (bubbles/drops) in agitated tanks has a scientific significance from the operational and design stand points with further investigations still required [1,2].

The time taken by the motion of the bubble in a turbulent field plays an important role in affecting the breakup rate, and consequently it affects the rates of mass and heat transfer. The length of time a bubble stays in the impeller zone can result in more fragmentation of bubble due to the longer exposure to high turbulence levels and shearing effects. The bubble retention close to the impeller, has been observed and discussed by some previous works [3–5]. It has been found that the retention interval is influenced by the hydrodynamics in the impeller vicinity. Studies reporting the experimental determination of residence time and its effect on the fluid particle breakup is currently limited in literature. The structures of flow current in the impeller region have been studied by several authors[e.g. 6–8]. Those studies indicated the complexity of the hydrodynamics around the impeller which results in an unpredictable dynamic behavior of fluid particles.

The stirred tanks breaks the gas bubbles (or drops) into smaller bubbles. This entrainment increase the residence time and interfacial aera between the gas and liquid, thereby allowing more mass (or heat) transfer into the process [9]. The breakage location is directly related to the time spent by the bubble in the impeller region. The time interval of each bubble staying in the impeller region causes the bubbles to spend more time exposed the turbulent eddies and shear forces provided by the impeller [1,10]. This can increase the BP and number of fragments. This time was observed to be dependent on the stirring speed (or Re), initial bubble size, and impeller geometry [5,11,12] .

The breakage time in this investigation is considered to be the time between the beginings of the bubble's deformation to the instant that the bubble has produced the final number of fragments, e.g. the final breakage has occurred [4,13,14]. Several authors [15–19] proposed that the breakage time is the time taken from initial deformation to the instant of the occurrence of first breakage which is called the initial breakage time.

The results obtained from single bubble breakage experiments are proved to be successful in understanding the behavior of bubbles of a particular size distribution [9]. Experimental determination of breakage time of a bubble in the impeller region using high speed imaging helps to better understanding the breakage dynamics occurring in stirred tanks.

The impeller design has an important influence on the breakage rate as it affects the intensity of turbulence and energy dissipation rate in the impeller region leading to affect the local breakages [20–22]. The breakage behavior of the bubble is affected by the design of the impeller as this design feature determines the flow patterns within the tank [23]. The impeller geometry also affects the shear stress exerted on the fluid particle and the energy dissipation rate, and thus, it affects the breakage rate depending on the operational parameters such as stirring speed and the fluid's physical properties. In addition, the impeller geometry influences the bubble's trajectory in the tank, the probability of collision with the blade(s) and the breakage rate [11,24]. The impeller geometry also affects the length of time the bubble remains close to the impeller by influencing the strength of the turbulent eddies and flow currents that may retain the mother bubble. in the high turbulence level region producing more daughter bubbles.

This current work follows on from Alabdaly et al [11] who studied and presented the effects of impeller geometry on the breakage rate for different stirring speeds (Re). This current work presents an investigation to determine the breakage time of the single bubble for the same impeller geometries and stirring speeds presented earlier under different operating conditions.

The breakage time in this investigation is considered to be the time between the beginings of the bubble's deformation to the instant that the bubble has produced the final number of fragments, e.g. the final breakage has occurred [4,13,14].

2. Experimental setup

Figure 1 shows a sketch of the apparatus. The experimental rig has been described in detail in Alabdaly et al, [11]. Briefly, the rig comprised a cylindrical tank made from Perspex, which is filled with the continuous phase (water). The cylindrical tank is surrounded by an outer rectangular Perspex tank, again filled with water to avoid the light reflections and distortion that can affect the quality image produced. The other equipment used during the experiments include a high-speed camera (Phantom, Miro C110), a mechanical stirrer, an impeller (three geometries), an air compressor for injecting the mother bubble, a LED illumination, control valve for controlling the injection rate of mother bubbles, and a Teflon tube for air injection to the tank. The frame rate of the high-speed camera was set to 1000 fps, which was founf enough to capture the bubble breakage around the impeller at a resolution of 1280 × 800. Three different impeller geometries were used, 4-Twisted blades impeller, 2-Flate blades impeller, and a 4-Flate blades impeller (details of the dimensions of each impeller and photos are presented in Alabdaly et al [11].

Three values of agitation speed were investigated; 180 rpm, 290 rpm, and 400 rpm. The corresponding values of Reynolds numbers (Re) are 18380, 26900, and 40830 which are calculated using [25,26]:

$$\mathrm{Re_i} = \frac{\rho N D_i^2}{\mu} \tag{1}$$

where, Di is the impeller's diameter, ρ is the density of the continuous phase, μ is the viscosity of continuous phase, and N is the stirring speed (rev/s).

The experimental procedure has been described in detail in the previous work [11]. Briefly, the mother bubble is released below the impeller by a distance of 70 mm. The injection location is 50 mm away from the tank's wall. The mother bubble is injected at a position below the impeller ensuring that the released bubble passes through the impeller region. The mother bubbles were injected at a rate of 1 bubble per 4 seconds. A glass tube was used to surround the injection tube to guarantee the released bubble was the same size for all Re. The average diameter of the mother bubbles for all Re, was measured to be 4.5 mm ±0.2 mm.

The motion of the injected bubble was recorded using a high-speed camera. The recording was then used to obtain the initial breakage time and final breakage time for each geometry and Re. For each condition investigated, at least 500 injection tests were conducted. This was sufficient for obtaining results of statistical significance. The breakage probability (BP) was via [27]:

$$\mathrm{BP}\ \% = \frac{\mathrm{n}}{\mathrm{n_T}} \times 100 \qquad (2)$$

The used high speed camera provides fast recording ability to record the events during the fast motion in impeller zone. These videos, using the software provided for this camera, can be played very slowly to analyze the motion and the breakage behavior. Besides, this camera provides a time record to a digit 10-9 from the second. From this time record, accurate time measurements can be obtained. Table 1 presents the uncertainty of experimental parameters.

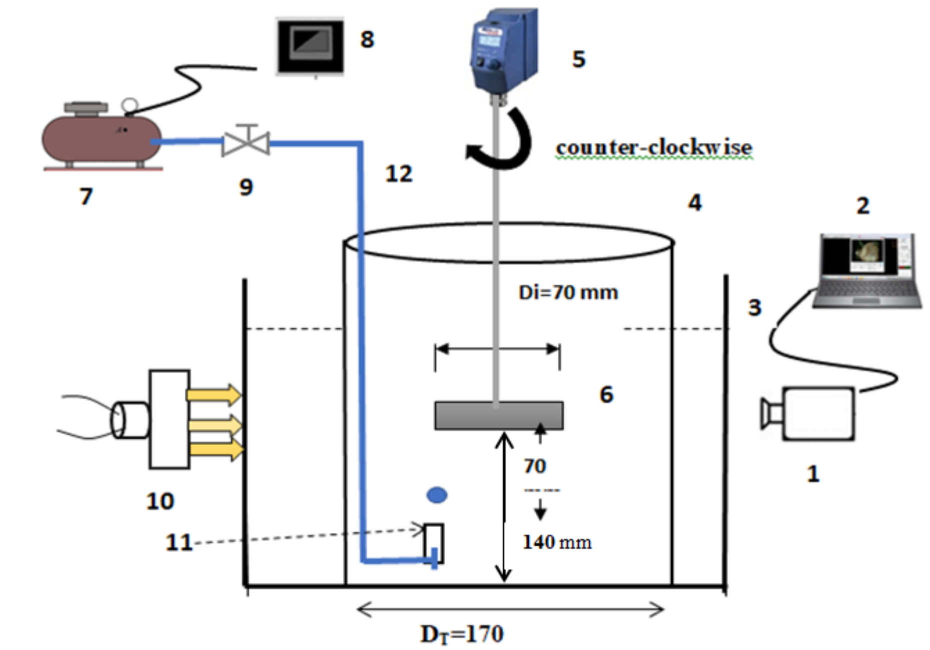

Figure 1: Experimental Fig, (1)phantom camera (high speed) (2) personal computer, (3) perspex tank, (4) internal perspex tank, (5) agitator, (6) perspex impeller, (7) regulator, (8) compressor, (9) control valve, (10) light projector, (11) framing tube, (12) Teflon tube [11].

Table 1: Experimental variables and results uncertainty.

Parameter	Deviation%
Re	±1.6%
Breakage time, ms	±15.5%
breakage probability	± 11.1%
Room temperature, ºC	± 1.0 ºC

3. Results and Discussion

3.1 The Breakage probability (BP)

Figure 2a shows the trends of BP with Re for the three impeller geometries investigated based on the results of the authors' previous work [11]. It can be seen that, for the three impeller types, there is a noticebale increase of PB with Re. The 4FB impeller gives highest value of BP, while 4TB impeller gives the lowest. The high breakage probability of 4- Flat blades impeller (4FB) is attributed to the high collision rate of bubbles with the blades and due to strength of turbulent fluctuations provided by this geometry and high shearing effect[11].

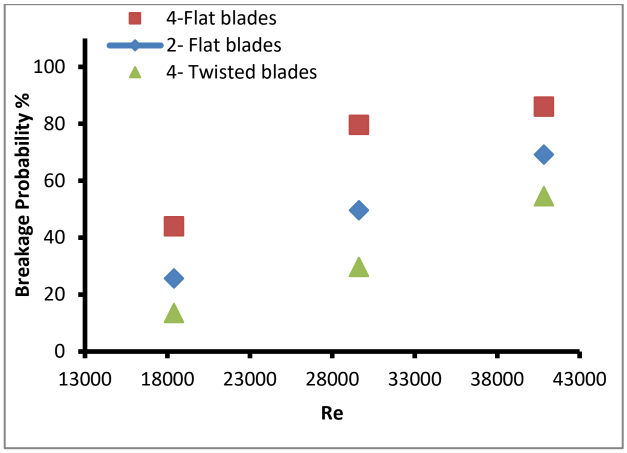

Figure 2a. BP vs. Re for different impeller geometries [11].

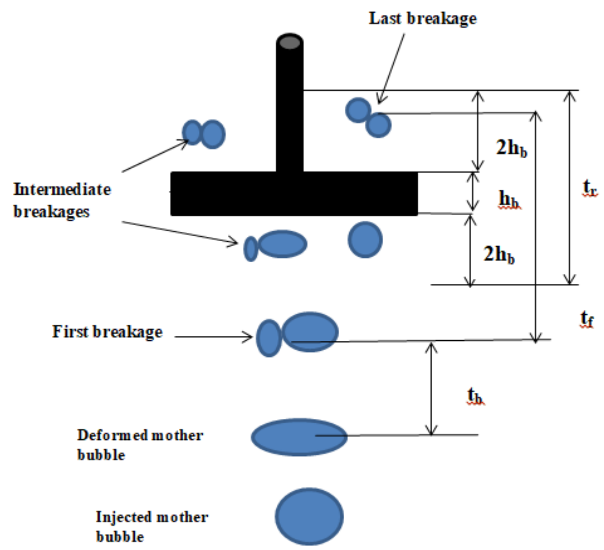

Figure 2b: Different time intervals for bubble breakage events, t_b is the breakage, t_f the breaking interval, and t_r is the retention time.

3.2 Breakage time

The breakage time (t_b), in this work, is adopted to be the time between the moment when the the bubble deforms by 10% and the moment of the occurrence of first breakage [10]. The interval between the oocurence of first breakage and last breakage, which includes generation of more daughter bubbles, is considered the breakaing interval (t_f). During this interval the bubble undergoes further breakages that produce the final population of fragments (daughter bubbles). The videos show that at a relatively high Re, the bubbles are retained close to blades for an more time. The "retention time" (t_r) of the bubble close to the blades, where the energy dissipation rate is high, is noticed to be an important factor that allows continuous breakup due to the longer exposure of the daughter bubble to the influence of high energy turbulent eddies. This region has been reported to be at a distance of about two blades height from the impeller blade [6]. Figure 2b presents a sketch showing the breakage intervals during the bubble's motion from the release point until leaving the "impeller region".

Figures 3a through 3c presents some typical images showing bubble breakage times for different Re for the 2FB impeller. It is evident from Figure 3a that the breakage time is 153.3 ms at Re=29600 for 2FB impeller. While Figure 3b for Re=40830 the time taken until the occurrence of first breakage is 87.7 ms and that of last breakage is 154.4 ms. Figure 3c, shows the breakage time for the 4TB impeller is 174 ms. It was observed that the 4-Twisted blade impeller gives longer breakage time than the other geometries.

Figure 4 presents the average breakage time (taken for at least 100 breakage events) versus Re for the different impeller geometries. It is clear that when Re increases, the the breakage time decreases for the three geometries. This is in agreement with the reported results of Kenno et al [28] and Hasan and Krakau [10]. In addition, the 4FB impeller gives the lowest average breakage time and the 4TB impeller gives the highest average breakage time. The decrease in breakage time with increasing Re is ascribed to the increase in turbulence strength and therefore increased rates of bubble collision with the turbulent flow structures.

The low values of breakage time for 4FB impeller is ascribed to the high shearing effect and turbulence level provided by this geometry of four flat blades [11]. The high increased interaction between bubbles and blades, including bubble –blade collision, plays an important role in reducing the time taken between the bubble's deformation stage and the occurrence of first breakage, i.e. the breakage time.

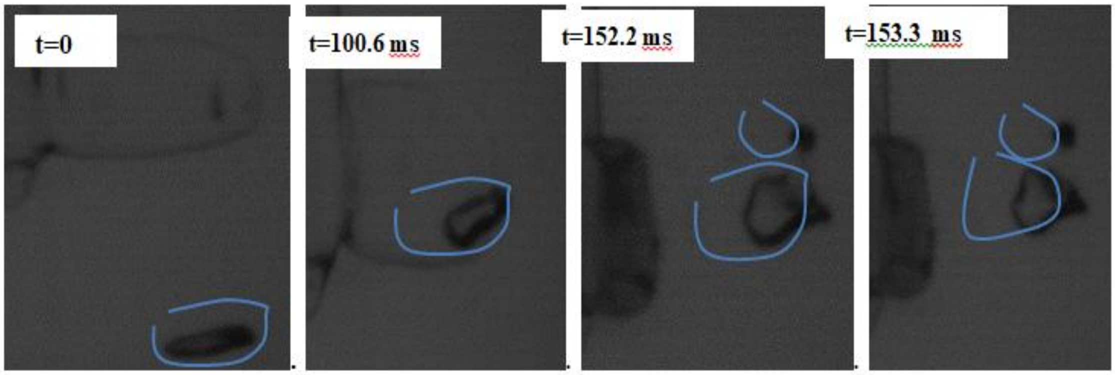

Figure 3a: Breakage time for Re=29600, 2FB impeller.

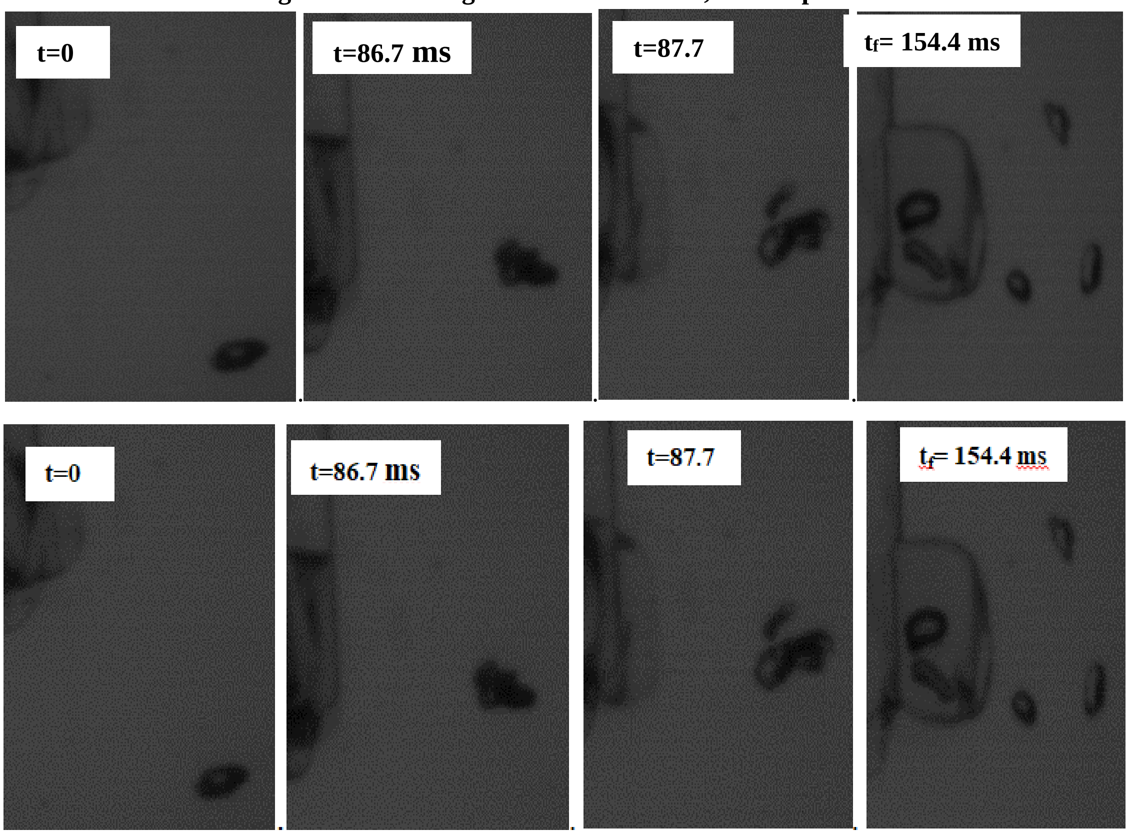

Figure 3b: Breakage time for Re=40830, 2FB impeller.

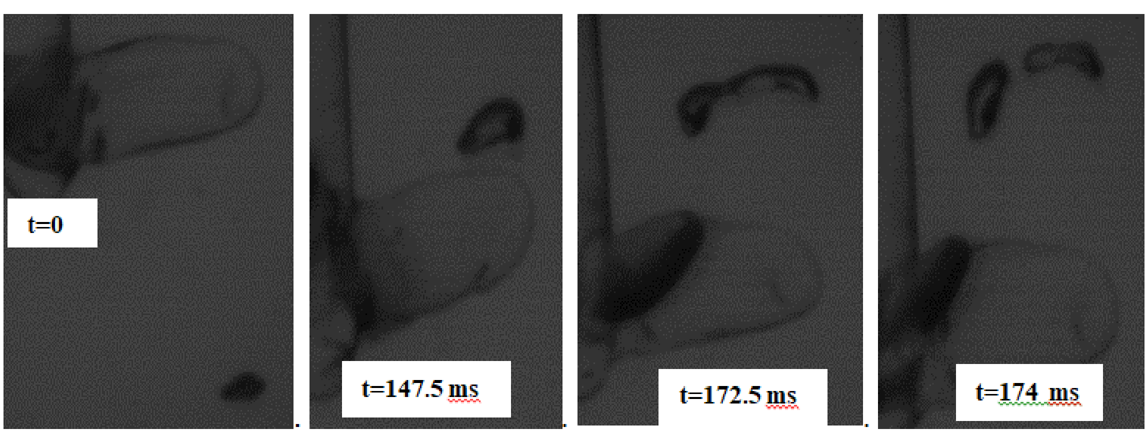

Figure 3c: Breakage time for Re=40830, 4FB impeller.

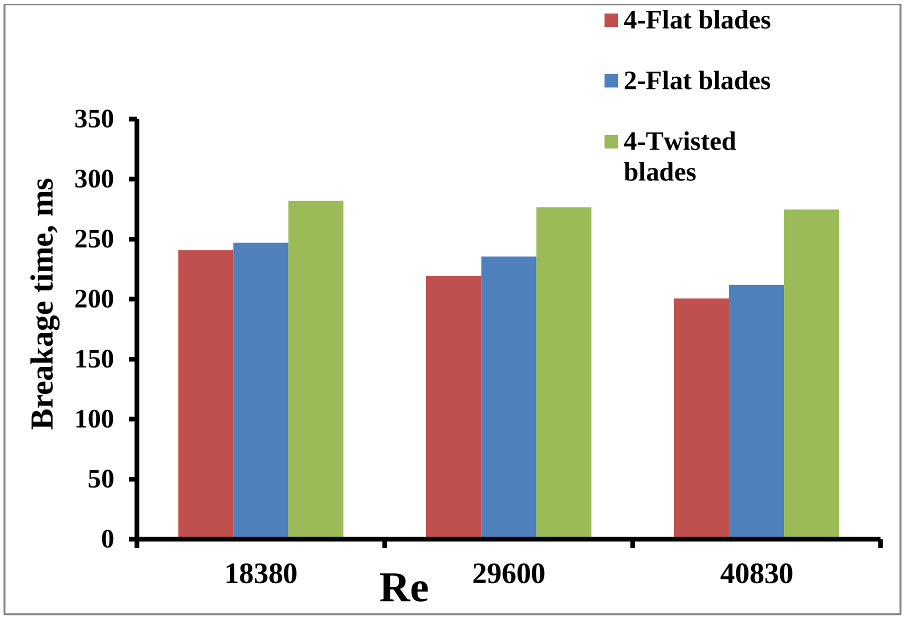

Figure 4: Breakage time vs. Re for three geometries.

3.3 Breaking time interval

The breaking interval, which is time duration taken between the first and last breakages, is function of Re [4]. This time interval includes the generation of more "daughter bubbles" due to the further breakups of the large fragments. The fragmentation persists until the daughter drops are no longer able to break up further due to their small size. Then, the daughter bubbles leave the impeller region due to bouncy forces.

In the current work, the results showed that the duration of this breaking interval is influenced by impeller geometry too. Images in Figures 5 through 7 present some photos as examples for the time taken by the bubble motion from first to last breakage in the impeller region. In these figures the time zero (t=0) is considered to be the time of first breakage. During this time interval more daughter bubbles are produced depending on Re and on the impeller type. The series of images in Figure 5a show that the time between first and last breakage is 27.5 ms in which 6 daughter bubbles are produced for the 2FB impeller at Re=40830. Figure 5b for the same conditions, 4 daughter bubbles are produced in 107.5 ms. So, this time interval is a subject of large variance because of the complicated hydrodynamics in the impeller zone which may drive the bubble into a region of either high or low energy level resulting in a short or long interval respectively.

Figure 6a presents a some selected of images for bubble breakage around the 4FB impeller with a breaking interval of 62.5 ms during which 9 fragments are produced (one fragment went behind the blades). Figure 6b shows that 7 fragments are produced in breaking interval of 77.5 ms. Figures 7a shows that for 4-Twisted blade 3 fragments are produced in 27.5 ms and Figure 7b shows that 5 fragments are produced in 42.5 ms.

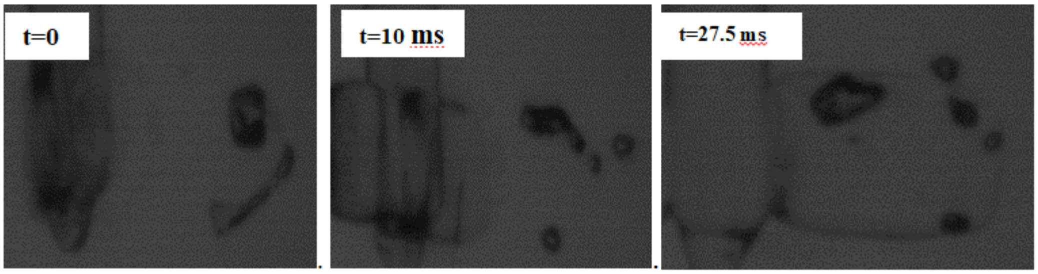

Figure 5a. Fragmentation into 6 daughter bubbles of 2-Flat blades impeller in 27.5 ms, Re=40830.

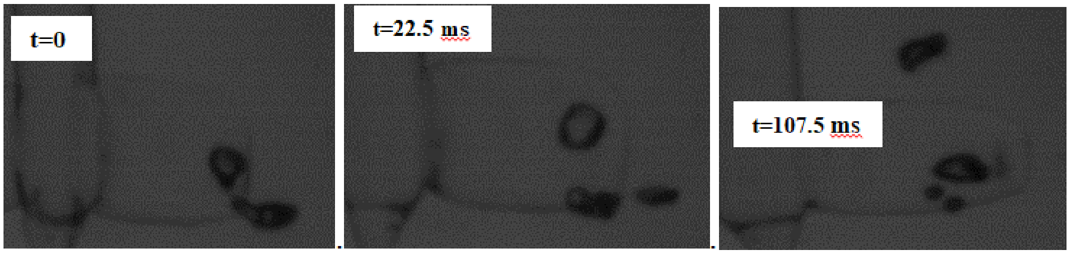

Figure 5b. Fragmentation into 4 daughter bubbles of 2-Flat blades impeller in 107.5 ms, Re=40830.

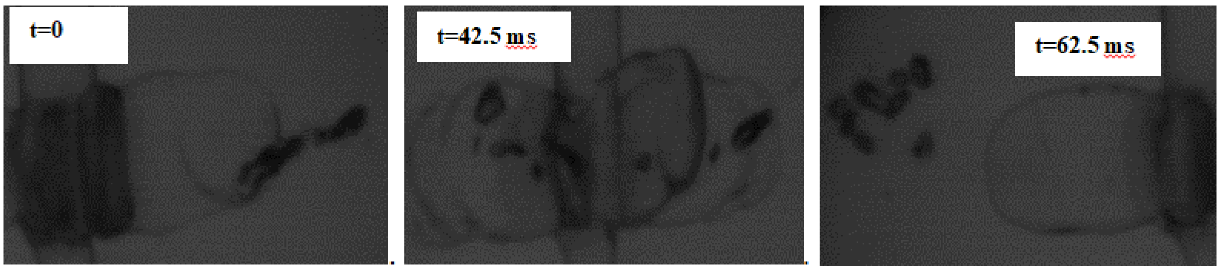

Figure 6a. Fragmentation into 9 daughter bubbles of 4-Flat blades impeller in 62.5 ms, Re=40830.

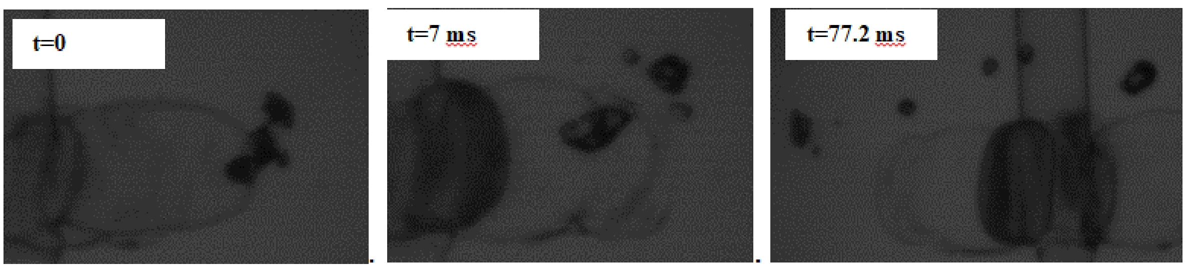

Figure 6b. Fragmentation into 7 daughter bubbles of 4-Flat blades impeller in 77.2 ms, Re=40830.

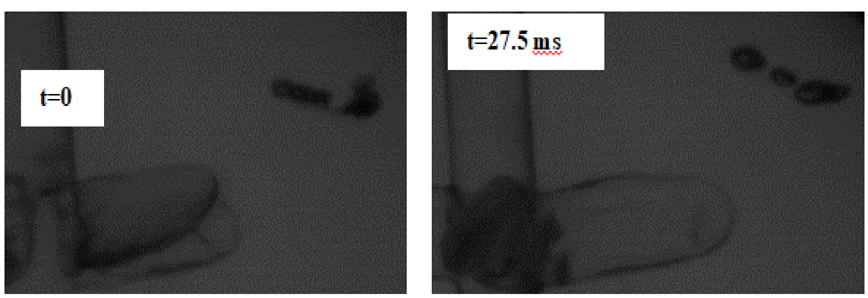

Figure 7a. Fragmentation into 3 daughter bubbles of 4-Twisted blades impeller in 42.5 ms, Re=40830.

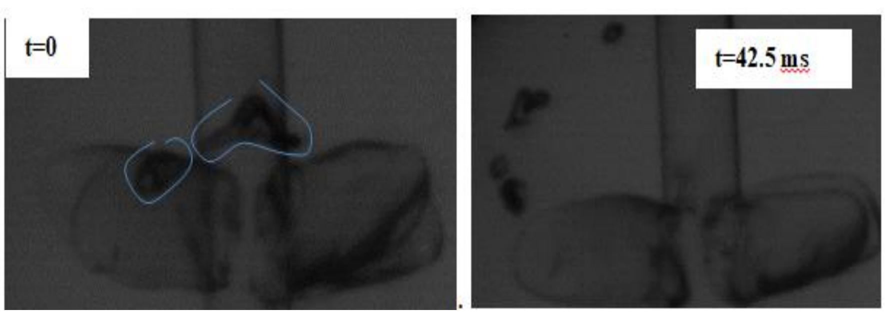

Figure 7b. Fragmentation into 5 daughter bubbles of 4-Twisted blades impeller in 42.5 ms, Re=40830

Figure 8 presents the average value of "breaking interval" aginst Re for the three geometries. It is evident that this interval increases with Re for the three geometries. For 2FB it increases by about 78% when Re increases from 18380 to 40830. This increase is because at higher Re, the bubble is caught by the rotating flow currents around the impeller resulting in a prolonged time exposed to turbulent eddies and shear forces [1,5]. Therefore, more daughter bubbles are produced during this time interval. Figure 8 also reveals that the breaking interval is highest for the 2FB impeller, followed by the 4FB impeller, and then the 4TB blades impeller. The high breaking interval for the 2FB blades and 4FB blades impeller is because these geometries cause complicated hydrodynamics in theimpeller region which retain the bubble for a prolonged time resulting in further fragmentation. The low breaking interval for the 4TB blade geometry is ascribed to the fact that the daughter bubbles leave the impeller region quickly compared to the other geometries. In other words, the retention time for this geometry is low as the flow patterns around the impeller do not hold the bubbles for prolonged time. Table 3 lists the values of retention time of the different geometries measured by high speed camera. This time is considered to start from the first breakage events until the departure of last daughter bubble from the impeller region.

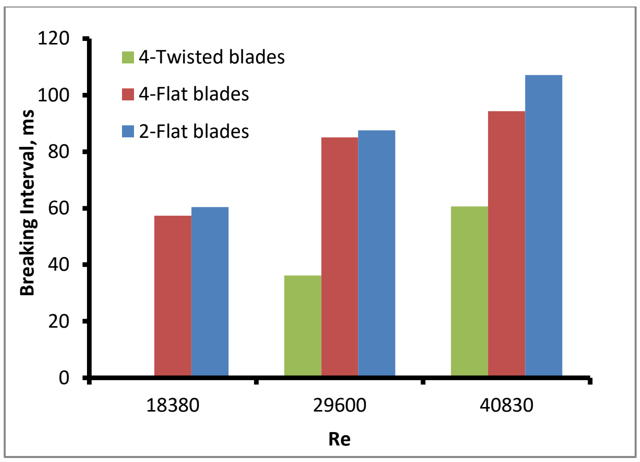

Figure 8: Breaking interval for different impeller geometries.

"Retention time" is an important factor that was observed to be affecting the bubble breakage rate which is found to vary with the impeller geometry and Re. It affects the breakage rate by allowing the daughter bubbles to be exposed to the impeller impact for a prolonged time. This permits the birth of more daughter bubbles especially from large size initially formed daughter bubbles. Table 4 lists the values of retention times for the average of at least 70 breakage events for each condition except for 4TB blades at lowest Reynolds numbe (Re), where the multiple breakages are few and thus, not statistically significant.

In general, the retention of a bubble for a certain time interval in the impeller zone for the case of the 4FB , results in a large number of daughter bubbles compared to 2FB and 4TB due to the longer exposure to the effect of high energy turbulent eddies.

It is evident from Table 2 that the retention time is influenced by the impeller geometry and it increases clearly with increasing Re for all geometries. The increase with Re is due to the increased turbulent motion of flow currents and the formation vortices that catch the bubbles in the vicinity of the impeller. In general, this delay in bubble motion in the high energy region causes the production of further daughter bubbles before all bubbles leave the impeller region. But, the further fragmentation of daughter bubbles during this time interval is also dependent on the strength of flow field and the size of the initially formed daughter bubbles; that will behave as mother bubbles for the subsequent breakages. The hydrodynamical effects around the impeller appear to causes the bubbles to approach the blade's tip which increases the probability of further breakage.

Table 2. Retention time for the used impellers at various Re.

Geometry	Retention time, ms		
	Re=18380	Re=29600	Re=40830
2FB	68.4	96.5	117.1
4FB	64.4	93.0	103.3
4TB	-	40.2	66.6

3.4 Birth rate of daughter bubbles

The average number of "daughter bubbles" produced during the breaking time interval for each geometry is presented in Table 3. It can be seen that the highest number of daughter bubbles is produced by the 4- Flat blade impeller, followed by the 2FBand then the 4TB. Dividing the number of fragments by the breaking time interval gives the average birth rate of the daughter bubbles, which are presented in Figure 9. It can be seen that the highest birth rate of daughter bubbles is for the 4FB impeller while the lowest is for the 4-Twisted blades impeller. This indicates that the 4FB impeller has the most efficient geometry in causing bubble breakage and fragmentation.

Table 3. Number of fragments (average) different geometries

Re	2FB	4FB	4TB
18380	2.4	2.66	2.19
29600	6.57	6.80	2.44
40830	8.79	10.1	4.30

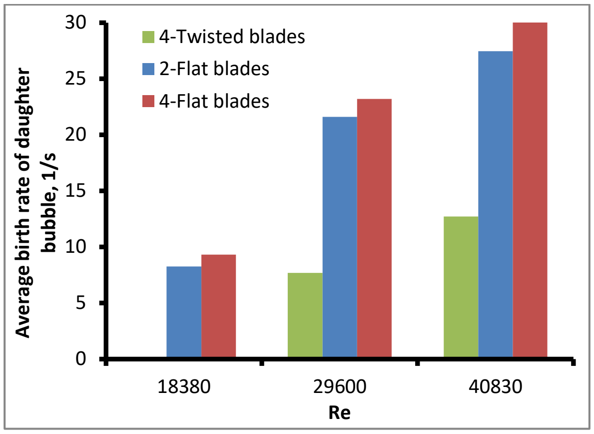

Figure 9. Birth rate of daughter bubbles vs. Re for different geometries.

The high birth rate for the 4FB impeller is attributed to the increase of probability of bubble's shearing off and then colliding with the blade(s). With the relatively long retention time caused by the 4FB impeller, the number of generated fragments increases compared to the other impeller geometries. It is to be noted that the 4FB gives the lowest bubble retention time. This is because the structure of flow field around this impeller does not retain the bubbles for long time and therefore fewer daughter bubbles fragments are made.

4. Conclusions

When a bubble travels in a turbulent field in a stirred tank, it's breakage experiences three time intervals. The first interval is between the initial deformation until the occurrence of first breakage event, which is considered to be the "initial breakage time". The second time interval is between the "first breakage" until the very last breakage which is considered to be the "breaking interval". There is a third time interval in which the bubble is caught and retained by flow currents around the impeller, which is considered to be the "retention time". This retention time starts when the bubble enters the impeller region until the departure of last daughter bubble from this region, which is below and above the impeller by twice the blade height. All of the three time intervals are a function of both Reynolds number and impeller geometry. For all impeller geometries, the breakage time decreases with increasing Re due to the increased interaction between the bubbles and the turbulent eddies in the flow field. The breaking interval and retention time increase with increasing Re because the flow currents around the impeller retain the bubble for a prolonged time close to the impeller. The 4FB impeller provides lower breakage time than 2FB and 4TB blades impellers due to the high energy dissipation rate produced by this impeller. The highest decrease is for 4FB impeller which is 20%, indicating the effcetivness of this geometry. The 2FB impeller produces a longer breaking interval due to the longer retention time in the near impeller region. For this impeller the breaking interval increases by 65% when Re increases to 40830. The 4FB blades impeller produces the highest birth rate of daughter bubbles (34 fragments at highest Re), therefore, it is the most efficient impeller geometry investigated in current work. 4TB impeller, is lowest birth rate of daughter bubbles indicating the low mixing effecincy.

Acknowledgment

The support from "Alexander von Humboldt Foundation/ Germany" to this work is appreciated

Symbols

μ	viscosity, kg/m s
D_i	Impeller diameter, m
N	rotational speed, rpm
Re	Reynolds number
T	time, s
ρ	density, kg/m^3

Abbreviations

2FB	two flate blades
4FB	four flate blades
4TB	four twisted blades
BP	Breakage probability

References

1. B.O. Hasan, M. F. Hamad, H. Sh. Majdi, M. M. Hathal, Experimental characterization of dynamic behavior of single bubble breakage in an agitated tank, European Journal of Mechanics / B Fluids .85 (2021) 430–443. https://doi.org/10.1016/j.euromechflu.2020.11.001

2. H. Zhou, X. Yu, B. Wang, S. Jing, W. Lan, S. Li, Experimental study on drop breakup time and breakup rate with drop swarms in a stirred tank,

AIChE J. 27(2021) 1–21. https://doi.org/10.1002/aic.17065

3. R. Andersson, B. Andersson, Modeling the breakup of fluid particles in turbulent flows ,AIChE, J. 52(2006) 2031–2038. https://doi.org/10.1002/aic.10832

4. B.O. Hasan, Experimental study on the bubble breakage in a stirred tank Part 1: Mechanism and effect of operating parameters, International Journal of Multiphase Flow 97(2017a) 94–108. https://doi.org/10.1016/j.ijmultiphaseflow.2017.08.006

5. B.O. Hasan, Experimental study on the bubble breakage in a stirred tank, Part 2: local dependence of breakage events, Exp. Therm. Fluid Sci. 96 (2018)48–62. https://doi.org/10.1016/j.expthermflusci.2018.02.013

6. H. Hartmanna, J. J. Derksen, C. Montavonb, J. Pearsonb, I. S. Hamillb, van den Akker H E A. Assessment of large eddy and RANS stirred tank simulations by means of LDA, Chem. Eng. Sci. 59 (2004)2419–2432. https://doi.org/10.1016/j.ces.2004.01.065

7. A. Zamiri, J. T. Chung, Numerical evaluation of turbulent flow structures in a stirred tank with a Rushton turbine based on scale-adaptive simulation Computers & Fluids 170(2018)236–248. https://doi.org/10.1016/j.compfluid.2018.05.007

8. J. Ramírez-Cruz, M. Salinas-Vázquez, G. Ascanio, W. Vicente-Rodríguez, C. Lagarza-Córtes, Mixing dynamics in an uncovered unbaffled stirred tank using Large- Eddy Simulations and a passive scalar transport equation, Chemical Engineering Science, 222(2020)115658. https://doi.org/10.1016/j.ces.2020.115658

9. M. S. N. Oliveira, A. W. Fitch, X. NI. A study of bubble velocity and bubble residence time in a gassed oscillatory baffled column, Effect of Oscillation Frequency, Trans IChemE, Vol. 81, Part A, (2003) 233-242. https://doi.org/10.1205/026387603762878692

10. B.O. Hasan, F. Krakau, Experimental study on the bubble breakage in a stirred tank. Part 1. Mechanism and effect of operating parameters Int. J. Multiph. Flow 97(2017) 94–108. https://doi.org/10.1016/j.ijmultiphaseflow.2017.08.006

11. H.A. Alabdly , H. Sh. Majdi, M. F. Hamad, M. M. Hathal, B.O. Hasan, Effect of impeller geometry on bubble breakage and the contributions of different breakage mechanisms in a stirred tank, Fluid Dyn. Res., 52(2020) 1–24. https://doi.org/10.1088/1873-7005/abbe97

12. E. Herø, H. Forgia, J. Solsvik, H. A. Jakobsen, Single drop breakage in turbulent flow: Statistical data analysis, Chemical Engineering Science: X8(2020) 100082. https://doi.org/10.1016/j.cesx.2020.100082

13. Maluta, F., Hydrodynamics, power consumption and bubble size distribution in gas-liquid stirred tanks, Chemical Engineering Research and Design, 194 (2023) 582–596. https://doi.org/10.1016/j.cherd.2023.05.006

14. J. Solsvik, H. Jakobsen, Single drop break up experiments in stirred liquid–liquid tank, Chem. Eng. Sci. 131 (2015a) 219–234. https://doi.org/10.1016/j.ces.2015.03.059

15. V. Hancil, V. Rod, Break-up of a drop in a stirred tank, Chem. Eng. Process. 23(1998) 189–193. https://doi.org/10.1016/0255-2701(88)80015-1

16. S. Maass, A. Gabler, A. Zaccone, A. Paschedag, M. Kraume, Experimental investigations and modeling of breakage phenomena in stirred liquid/liquid systems, Chem. Eng. Res. Des. Trans. IChemE A 85 (A5) (2007) 703–709. https://doi.org/10.1205/cherd06187

17. M. Stork, Model-based Optimization of the Procedure of Emulsification, PhD thesis, Technical University Delft, Netherlands, 2005.

18. S. Maass, M. Kraume, Determination of breakage rates using single drop experiments, Chem. Eng. Sci. 70 (2012) 146–164. https://doi.org/10.1016/j.ces.2011.08.027

19. Y. Shuai, X.Wang, Z. Huang, J. Sun, Y. Yang, Experimental measurement of bubble breakup in a jet bubbling reactor, AIChE Journal, 67(2021) 1. https://doi.org/10.1002/aic.17062

20. M. Martin, F. Montes J, M. Gal'an, Bubbling process in stirred tank reactors I: agitator effect on bubble size, formation and rising Chem. Eng. Sci.

63 (2008a) 3212–3222. https://doi.org/10.1016/j.ces.2008.03.028

21. B. Prakash, T. S. Milinkumar, V. K. Pareek, R. P. Utikar, Impact of HSPBT blade angle on gas phase hydrodynamics in a gas–liquid stirred tank, Chemical Engineering Research and Design 130 (2018)219–229. https://doi.org/10.1016/j.cherd.2017.12.028
22. D. Mesa, R. Pablo, Brito-Parada, Bubble size distribution in aerated stirred tanks: Quantifying the effect of impeller-stator design, Chemical Engineering Research and Design 160(2020) 356–369. https://doi.org/10.1016/j.cherd.2020.05.029
23. M. Martin, F. Montes, M. Galan, Influence of impeller type on the bubble breakup process in stirred tanks, Ind. Eng. Chem. Res. 47(2008b) 6251–6263. https://doi.org/10.1021/ie800063v
24. C. Bliatsiou, A. Malik, L. Böhm, M. Kraume, Influence of Impeller Geometry on Hydromechanical Stress in Stirred Liquid/Liquid Dispersions, Ind. Eng. Chem. Res., 58(2019) 2537−2550. https://doi.org/10.1021/acs.iecr.8b03654
25. S. M. Harriott (). Unit Operations of Chemical Engineering 6th ed., McGraw-Hill International, New York, 2001.
26. B.O. Hasan, M.A Sahir.. Corrosion of carbon steel in two phase flow (CO2 gas-CaCO3 solution) controlled by sacrificial anode, Journal of Natural Gas Science and Engineering, 46(2017) 71-79. https://doi.org/10.1016/j.jngse.2017.06.032
27. C.A. Coulaloglou, L.L. Tavlarides, Description of interaction processes in agitated liquid–liquid dispersions. Chem. Eng. Sci. 32 (11) (1977) 1289–1297. https://doi.org/10.1016/0009-2509(77)85023-9
28. M. Konno, A. Aoki, S. Saito, Scale effect on breakup process in liquid-liquid agitated tanks. J. Chem. Eng. Jpn. 16 (4) (1983) 312–319. https://doi.org/10.1252/jcej.16.312